INFOCOM17 WKSHPS WCNEE 2017 1570336759

A Cooperative Raman Spectrum Reconstruction Platform for Real-time In-vivo Nano-biosensing

Hongzhi Guo, Zhi Sun, and Josep Miquel Jornet

State University of New York at Buffalo, Buffalo, NY, USA
{hongzhig, zhisun, jmjornet}@buffalo.edu

***Abstract*—In the last few decades, the development of miniature biological sensors able to detect and measure different phenomena at the nanoscale has led to transformative disease diagnosis and treatment techniques. Among others, biofunctional Raman nanoparticles have been utilized in-vitro and in-vivo for multiplexed diagnosis and detection of different biological agents. However, existing solutions require the use of bulky lasers to excite the nanoparticles and similarly bulky and expensive spectrometers to measure the scattered Raman signals, which limit the practicality and applications of this nano-biosensing technique. In addition, due to the high path loss of the intra-body environment, the received signals are usually very weak, which hampers the accuracy of the measurements. In this paper, the concept of cooperative Raman spectrum reconstruction for real-time in vivo nano-biosensing is presented for the first time. The fundamental idea is to replace the single excitation and measurements points (i.e., the laser and the spectrometer, respectively) by a network of interconnected nano-devices able to simultaneously excite and measure nano-biosensing particles. More specifically, in the proposed system a large number of nanosensors jointly irradiate and distributively collect the Raman response of bio-functional nanoparticles traveling through the blood vessels. This paper presents a detailed description of the sensing system and, more importantly, proves its feasibility, by utilizing accurate models for intra-body light propagation and nanoparticle scattering processes. The numerical results show that with a certain density of nano-biofunctional particles, the reconstructed Raman spectrum can be recovered and utilized to accurately extract the targeted intra-body information.**

***Index Terms*—Cooperative Raman spectroscopy, Signal estimation, Wireless intra-body communications, Wireless nanosensor network.**

I. Introduction

Driven by the development of nanotechnology, emerging novel nanosensors have been envisioned to provide unprecedented sensing accuracy for many important applications, such as food safety detection, agriculture disease monitoring, health monitoring, drug delivery, and genetic engineering, among others [1]–[3]. Since nanosensors can interact directly with the most fundamental elements in matter, e.g., atoms and molecules, its sensitivity is high and the detection is in real-time. One of the most promising applications of nanosensors is in-vivo biosensing [4], [5], where nanosensors are injected into human body to collect real-time information for disease detection and health monitoring. Most of the diseases can be treated at their early stages. Moreover, the information provided by nanosensors can help us understand diseases and bio-functions at very fundamental level and this can give more detailed information, which have never been found at the macroscopic level.

This work was supported by the US National Science Foundation (NSF) under Grant No. CBET-1445934.

The use of nanoscale communication techniques can enable data transmission among nanosensors. However, there are two fundamental limitations of directly using active nano-sensors in human body. First, on the one hand, wireless nanosensors require continuous power supply to support wireless data transmission and motion control. On the other hand, due to the limited size of the nanosensor, a large battery cannot be equipped and, even worse, recharging the battery is difficult. Second, the wireless nanosensor requires circuitry and antenna to process and radiate wireless signals, which further increases its size. In order to alleviate the side-effects caused by nanosensors in human body, we need to reduce its size by removing the battery and wireless components.

Metallic nanoparticles coated with Raman active reporter molecules have been widely used as surface enhanced Raman scattering labels for multiplexed diagnosis and bio-detection of DNA and proteins [6]. This is a promising solution since it does not require power and wireless components on the nanoparticles. Their motion can be driven by the dynamic fluids in human circular system and the information can be delivered by electromagnetic scattering. The Raman active reporter molecules can interact with chemicals inside human body and the incident single-frequency optical light can be scattered into a wide frequency band with unique power spectrum due to molecule vibration. Based on this unique spectrum, we can identify the molecules inside human body. The Raman active reporter molecules are placed on the surface of metallic nanoparticles to enhance the scattering efficiency in order to improve the detected power.

While this solution can dramatically reduce the size of the nano-device that is injected into human body, it still has limitations, which prohibit it from being widely used. First, a laser is needed to excite the engineered nanoparticle inside human body and a spectrometer is demanded to detect scattered Raman signal. Both the laser and the spectrometer are bulky and expensive and, thus, not portable and affordable. In addition, the accuracy of this sensing setup is not high enough since the scattered Raman signal is much weaker than the emitted signal by the laser due to the small scattering cross section of the nanoparticle and the dispersive and lossy propagation medium.

To address the aforementioned challenges, we propose the concept of cooperative Raman spectroscopy. The system consists of external nanosensors and internal nano-biofunctional particles. The bulky, expensive lasers and spectrometers are replaced with distributed nanosensors, which can both emit and detect optical signals, by leveraging the state of the art in nano-lasers and and nano-photodetectors [7]. The nanosensors

are placed on a smart ring, which can reduce the distance to the intra-body particles to increase the received signal strength. Moreover, by letting the nano-sensors distributed, we can increase the diversity of detection and optimally allocate resources to make the system more robust.

In this paper, we design a sensing system for cooperative Raman spectroscopy. By using nanosensors equipped with nano-emitters and nano-detectors, we first present the system architecture, where the processes of signal generation, scattering, and detection are introduced. Based on the operational framework, we provide theoretical models to describe each part of the system, including signal transmission, noise, nano-biofunctional particle density, and nanosensor's distribution. Different from wireless signal propagation in Radio Frequency (RF) band, the optical signal received by the detector subjects to a Poisson distribution and the signal is distorted by dark current noise. Moreover, the nano-biofunctional particles may also interact with unexpected molecules, which introduces more noises. Both of the two noises are taken into account in the system model. Next, we derive the expected detected power of each nanosensor using the stochastic system model. Based on the theoretical model and nanosensor observations, we provide a Raman signal estimation algorithm to reconstruct the spectrum. The numerical simulation validates the accuracy of the proposed estimation method.

The remaining part of this paper is organized as follows. The system architecture and operational framework are introduced in Section II. After that, we present the system model and describe the main factors that can affect the sensing performance in Section III. This is followed by the derivation of the expected detected power by each nanosensor and the signal estimation algorithm in Section IV. The proposed system performance is numerically evaluated in Section V. Finally, this paper is concluded in Section VI.

II. System Architecture and Operational Framework

The system architecture of cooperative Raman spectroscopy consists of three important units, namely, the external excitation and sensing system on a ring, the internal nano-biofunctional particles, and data fusion and processing unit. In the following, we first introduce the system architecture.

A large number of interconnected nanosensors are installed on a ring and each nanosensor has some nano-transceivers, which are able to both emit optical signal and detect electromagnetic scattering from the internal nano-biofunctional particles. The nanosensors are uniformly distributed on the ring. In this way, no matter how the ring is worn, it does not affect the detection accuracy. In addition, the nano-transceivers on a nanosensor emit signals in the same frequency, but detect signals at different frequency bands. The scattered signal from the particle occupies a wide spectrum. However, it is challenging to design a compact broadband nano-detector. Therefore, the detector is narrow-band and each detector measures the received signal power at a single frequency.

The nano-biofunctional particles coated with different dye or Raman active reporter molecules can be used as surface-enhanced Raman spectroscopy labels for multiplexed diagnosis and bio-detection of DNA and proteins with very high sensing specificity. A large amount of particles are injected into human circulatory system as a mixture with other bio-friendly solution. In the blood vessels, the particles meet with different kinds of molecules including those generated by the targeting diseases. Since different chemical reactions can generate different coat on the particles, once the particles are excited by the incident wave, the power would be scattered into different frequencies and a unique power spectrum can be created. Consequently, we can identify the molecules that the particles met in the blood vessels based on the spectrum. However, since particles may meet with many other unexpected molecules, the detected power may not solely come from the targeted molecules. In other words, the particles are contaminated and the scattered signal consists of noise caused by unpredictable molecules.

Once the raw spectrum data are collected by each sensor, there are two different ways to reconstruct the spectrum and detect the molecules. 1) As shown in Fig. 1(a), the first one is a centralized architecture, where the raw spectrum data are sent directly to a data fusion center to do further process and identification. This method can provide the most accurate results since all the raw data are considered in the detection algorithm. Also, the data fusion center can first compress the raw spectrum data and then send to the smart phone. In this way, the smart phone will perform spectrum reconstruction and molecule identification. However, there are two disadvantages, which can prevent us from applying this architecture. First, the communication overhead is significant since all the data need to be transmitted, which can increase the system delay and real-time detection may not be possible. The second disadvantage is that the signal processing in data fusion center requires a large amount of energy and computation resource, which increases the burden of the ring. 2) The second architecture relies on a distributed sensing concept as shown in Fig. 1(b). Each of the nanosensor performs detection algorithm and send the results to the data fusion center. Based on the local detection results, the data fusion center performs a global detection and send the detected results of the molecules to the smart phone. In this way, most of the data are processed locally and thus the communication overhead can be dramatically reduced. Nevertheless, this system requires more computation resources for the nanosensor and the detection accuracy may not be as accurate as the centralized system.

The operational framework of the cooperative Raman spectroscopy consists of three phases.

- First, the synchronized emitters on the ring radiate electromagnetic signals at the same frequency into a finger. The frequency has been selected to minimize the signal propagation loss in intra-body environment.
- Second, the flowing particles in blood vessels receives the radiated electromagnetic signal from one or many emitters. Then, the particles scatter the power into a wide spectrum.
- Lastly, the scattered signal propagates towards detectors and then the power at a specific frequency is detected. After that, one can use different data fusion and detection architectures as shown in Fig. 1(a), and Fig. 1(b) to process the sensed data, upon which the machine learning algorithms can be applied to identify the category of the molecules interacted with the particles.

III. System Model

Consider that there are N_s nanosensors uniformly installed on a ring and each nanosensor has N_f nano-transceivers.

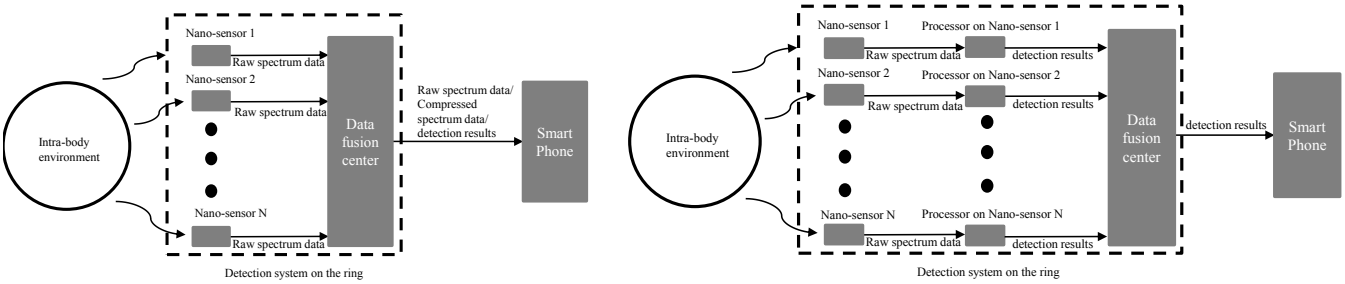

(a) Centralized detection system. All the sensors first send raw data to a data fusion center on the ring. Then, the data fusion center can either process or send the raw data to a smart phone.

(b) Distributed detection system. Each sensor can first sense and process the raw data and make its own decision based on its observation. Then, the detection results of each sensor will be sent to a data fusion center on the ring to do a global detection. Finally, the detection results are reported to a smart phone.

Fig. 1. Centralized and distributed detection system architecture.

Each nano-transceiver has one emitter and one detector. The whole Raman spectrum is divided into N_f sub-bands and each detector on the nanosensor detect signals in one sub-band. Note that due to the noise and low-density of nano-biofunctional particles, some detectors may not receive enough power and thus multiple nanosensors are employed to make the system reliable. Since the bone is a much denser medium than other layers of the finger, it can block the propagation of electromagnetic field at optical band. We assume both the finger and the bone are cylinders with radius r_f and r_b, respectively. The blood vessels, including artery, vein, and capillary, are randomly distributed between the skin and bone with density λ_b. In each blood vessel, the particles arrive with a density proportional to the area of the blood vessel's cross section, which is denoted by $\lambda_{par} = \lambda_0 s_b$, where λ_0 is the particle density of a unit area and s_b is the area of a blood vessel's cross section. In reality, λ_0 is a function of time. When the particles are injected into the circulatory system, λ_0 gradually increases. After a while, some of the particles are disposed by natural physiological actions and the density gradually decreases. In this paper, we consider the sensing is quasi-static since the optical light propagates much faster than nano-biofunctional particles' movement. Thus, in the following the particles are assumed to be static and the optical channel remains constant during the sensing period.

A. Signal Propagation Model

The optical signals have to penetrate skin, fat, and blood vessels to reach the nano-biofunctional particles. Extensive analytical and empirical models have been derived to capture this process [8]–[11]. There are many categories of cells and tissues and their properties vary from person to person. In [12], an analytical channel model for intra-body in-vivo biosensing is developed by considering the properties of individual cells. In this paper, we use the same model to describe the propagation loss of EM wave radiated by the emitters, which can be simply written as

$$h(f, d) = e^{-\mu(f)d}, \tag{1}$$

where $\mu(f)$ is the loss coefficient, d is the propagation distance and f is the operating frequency. Besides this large scale fading, due to the multipath effect caused by scattering, a Rayleigh fading coefficient is also considered whose scale parameter is σ.

B. Noise Model

The noise in a sensing system can deteriorate the detection results and significantly affect the sensing capability. In the cooperative Raman spectroscopy system, there are primarily two noises, namely, molecules noise and shot noise.

1) Molecules Noise: The nano-biofunctional particles flow through the circulatory system and interact with plenty of molecules. On one hand, they meet with the valuable molecules carrying information about diseases and then the important electromagnetic properties are changed on their surfaces. Through optical scattering, we can detect those molecules by identifying the power spectrum. On the other hand, the nano-biofunctional particles also encounter many unexpected molecules in intra-body environment. Although the particles are not designed to interact with these molecules, some chemical reactions can happen and change the particles' properties randomly, which are reflected in the received power spectrum. The original power spectrum is distorted by unexpected noise power. As a result, to accurately reconstruct the power spectrum, the molecule noise has to be taken into account.

Since the molecules in human body have a large variety of categories, which demonstrate different resonant frequencies in Raman spectrum, we can consider the noise power is the same for all the frequency bands. Therefore, the noise can be considered as white noise with uniform power across a wide band. Due to the large amount of molecules, the noise can be considered as positive and negative values and its distribution is Gaussian with mean value 0 and standard deviation σ_m. Consequently, the noise caused by molecules can be regarded as additive white Gaussian noise $\mathcal{N}(0, \sigma_m^2)$.

2) Shot Noise in Detector: The noise in the detector is mainly shot noise, whose power is given by

$$P^s = 2q\gamma_d \hat{P}^{dt} B_{sub} \tag{2}$$

where q is the electronic charge, γ_d is the detector's responsivity, $\hat{P}^{dt}$ is the total detected power of both signal and molecule noise, and B_{sub} is the sub-band bandwidth.

C. Particle Scattering Model

The nano-biofunctional particles first absorb power from emitters and then scatter the power with unique information. Therefore, the particles can be regarded as an information source, which sends encoded data to detectors, i.e., its scattering coefficients. As shown in Fig. 2, the scattered signal by

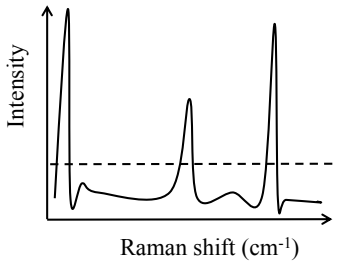

Fig. 2. Spectrum of Raman scattering.

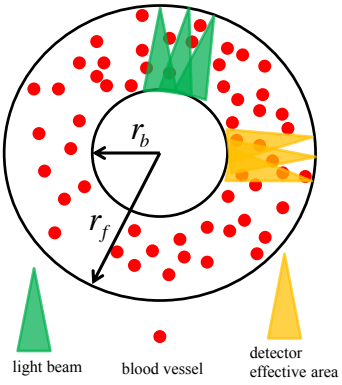

Fig. 3. Illustration of light beam and detector's effective area. The outer circle is the cross section of finger and the inner one is the cross section of bone.

the nano-biofunctional particle is spreaded on a wide spectrum with varied signal intensity. This spectrum is divided into sub-bands and the amplitude in each sub-band is considered as the transmitted signal. This power conversion consists of two steps. First, the received power by the particle at frequency f_t is absorbed. Then, the nano-biofunctional particle scatters the power into a wide frequency band. As a result, the scattering coefficient can be written as $\eta(f_t, f_i)$, where f_i is the center frequency of a sub-band.

D. Particle Arriving Model

The particles are injected into circulatory system with a certain density. They arrive at the target sensing area with a diluted density. To model this process, we consider the arrival rate of particles in a unit cross section of blood vessel is λ_0. Since different blood vessels have different cross section areas, their particles arriving rates are also different. Moreover, the process of particle moving is modeled as Poisson point process. The number of the particles that can be excited by the emitter depends on the position of the blood vessel, the distance to the emitter, and the density of the particles. The radiated electromagnetic field by an emitter can cover a three dimensional cone and each detector can receive the electromagnetic radiation from the same cone. As shown in Fig. 3, the blood vessels are homogeneously distributed between skin and bone. The emitter and detectors have their own effective area within which the gain is a constant. The number of blood vessels and nano-biofunctional particles within a cone are random, which depend on number of blood vessels and particle density. Also, particles can receive power from multiple beams. In this paper, we consider adjacent beams that are overlapped work in different time slots to eliminate the correlation among them, i.e., in each time slot the particles

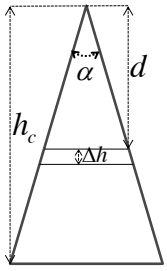

Fig. 4. Light beam and angle.

within a beam can only receive power from one emitter. Since the beam angles of the emitter and detector are small, we safely assume that all the points on the same horizontal line has the same distance to the emitter. To find the number of particles in a blood vessel and the received power, we need to find the distributions of the length of blood vessels within a cone and their distance to emitter. Given the blood vessel's effective length l, the number of particles within it is given as

$$\mathbb{P}(N_p = n | L = l, S_b = s_b) = \frac{(\lambda_0 s_b l/u)^n}{n!} e^{-\lambda_0 s_b l/u}, \quad (3)$$

where s_b is the cross section area of the blood vessel and u is the velocity of blood. We assume the cross section of the blood vessel is uniformly distributed in $[S_l, S_u]$ with a probability density function $f(s_b) = 1/(S_u - S_l)$.

IV. Raman Spectrum Estimation

Based on the system model, in this section we provide a method to reconstruct the Raman spectrum based on the detected signal power and priori knowledge of the signal propagation and system configuration. The estimation is based on the expected detected power. We derive the analytical model for it and then by averaging the multiple observations of nanosensors, we can find the scattering coefficients of the nano-biofunctional particle.

A. Expected Detected Power

It is worth noting that, since the bandwidth B_{sub} is small enough, the channel can be considered as flat fading within a sub-band. Also, our analysis is general and it holds for all the sub-bands. We first derive the expected detected power for one detector. Consider that there are N_p particles in one or several blood vessels covered by optical cone of both an emitter and associated detector. The expected detected power can be expressed as

$$\mathbb{E}(P^d) = \mathbb{E}(\sum_{i=1}^{N_p} P_i^d) \quad (4)$$

$$\approx \mathbb{E}(\sum_{i=1}^{R_s} \sum_{k=1}^{\hat{N}_{p_i}} P_{i,k}^d) \approx \sum_{i=1}^{R_s} \mathbb{E}(\hat{N}_{p_i}) \mathbb{E}(\hat{P}_i^d), \quad (5)$$

where P_i^d is the nano-sensor detected power scattered by the i^{th} nano-biofunctional particle, $\hat{N}_{p_i}$ is the nano-biofunctional particle number within the sub-region, and $\hat{P}_i^d$ is the expected detected power scattered by sub-region i. As shown in Fig. 4, we divide the cross section of the cone into sub-regions with height Δh. Then, we classify the nano-biofunctional particles into each sub-region based on their position and in this way (4)

can be approximated by (5). Here, the height Δh is considered as the average height of the blood vessel's cross section, which is $\Delta h = 2\sqrt{\frac{S_u+S_l}{2\pi}}$. Next, we look at each sub-region and find the expected detected power.

In each sub-region, we consider all the nano-biofunctional particles have the same distance to the detector since the beam angle of the emitter is very small. The expected nano-biofunctional number in a sub-region can be found by using

$$\mathbb{E}(\hat{N}_p) = \sum_{n=1}^{\infty} \Big[n\mathbb{P}(\hat{N}_p = n) \Big]. \tag{6}$$

Due to the complicated blood vessel distribution and their different cross section areas, here we consider an equivalent scenario, i.e., the randomly distributed blood vessels on a plane of the cone are considered as one equivalent blood vessel. The average length of a blood vessel in a sub-region can be expressed as

$$\hat{l} = \int_0^{d\tan\frac{\alpha}{2}} \frac{2\sqrt{(d\tan\frac{\alpha}{2})^2 - x^2}}{d\tan\frac{\alpha}{2}} dx = \frac{\pi d\tan\frac{\alpha}{2}}{2}. \tag{7}$$

The cross section of the equivalent blood vessel can be approximated by $\frac{S_u+S_l}{2}$ since the cross section is uniformly distributed. The expected number of blood vessels in a sub-region can be expressed as

$$\lambda_{eq} = \frac{\lambda_b d\Delta h\tan\frac{\alpha}{2}}{2r_f^2}. \tag{8}$$

Then, the length of the equivalent blood vessel is $l_{eq} = \hat{l}\cdot\lambda_{eq}$ and the probability that there are n nano-biofunctional particles in the equivalent blood vessel can be written as

$$\mathbb{P}(\hat{N}_p = n) = \frac{(\lambda_0 s_{eq} l_{eq}/u)^n}{n!} e^{-\lambda_0 s_{eq} l_{eq}/u}. \tag{9}$$

Next, the expected detected power from one particle at distance d is given as

$$\mathbb{E}(\hat{P}_i^d) = \mathbb{E}[P_t G_t(f_t) h^{tp} \eta(f_t, f_i) G_r(f_i) h^{pr}], \tag{10}$$

where P_t is the transmitted power by the light emitter, $G_t(f_t)$ is the gain of the light emitter at frequency f_t, h^{tp} is the light propagation loss from the emitter to the nano-biofunctional particle, h^{pr} is the light propagation loss from the nano-biofunctional particle to the detector, $\eta(f_t, f_i)$ is the scattering coefficient of the particle, and $G_r(f_i)$ is the gain of the detector. Since on the left-hand-side of (10) only h^{tp} and h^{pr} are random variables (they are functions of distance and subject to Rayleigh fading) and they are independent, (10) can be simplified as

$$\mathbb{E}(\hat{P}_i^d) = \frac{\pi}{2} P_t G_t(f_t) \eta(f_t, f_i) G_r(f_i) h^{tp}(f_t, d) h^{pr}(f_i, d) \sigma^2. \tag{11}$$

By substituting (9) and (11) into (5), we can obtain the expected detected power by a detector on a nanosensor.

TABLE I
NUMERICAL PARAMETERS

Parameter	Value	Parameter	Value
λ_b	10^6 /m^2	u	0.45 m/s
S_u	300 nm^2	S_l	3 nm^2
r_f	5 mm	r_b	2.5 mm
α	$\frac{\pi}{36}$	G_s	30 dBi
G_r	30 dBi	B_w	1 THz

B. Spectrum Reconstruction

To reconstruct the spectrum, we need to estimate the value of $\eta(f_t, f_i)$, which is the only unknown parameter in the expected detected power (4). As discussed in the noise model, besides the detected signal power, there are also molecule noise P^m and shot noise P^s. The overall detected power by the nanosensor can be expressed as

$$P^{od} = \gamma\eta(f_t, f_i) + P^m + P^s, \tag{12}$$

where $\gamma = \mathbb{E}(P^d)/\eta(f_t, f_i)$. A nanosensor observes a sequence of detected power $[\tilde{P}_1^{od}, \tilde{P}_2^{od}, \cdots, \tilde{P}_{N_o}^{od}]$ and the mean value is $\hat{P}^{od}$, upon which one can estimate the scattering coefficient. Since $P^m \sim \mathcal{N}(0, \sigma_m^2)$, the Maximum Likelihood (ML) estimation of $\eta(f_t, f_i)$ is

$$\hat{\eta}(f_t, f_i) = \frac{\hat{P}^{od} - P^s}{\gamma}. \tag{13}$$

In this way, each detector can estimate the scattering coefficient at its own operating frequency. Based on the estimated coefficients, we can reconstruct the Raman spectrum. However, there are two primary factors that can strongly affect the accuracy of the estimation, i.e., the noise and nano-biofunctional particle density. To evaluate the performance of the spectrum reconstruction, we use the normalized mean square error $\sum_{i=1}^{N_f}[1 - \frac{\hat{\eta}(f_t,f_i)}{\eta(f_t,f_i)}]^2/N_f$ as a metric to evaluate the effect of both noise and particle density.

Since the density of the nano-biofunctional particle is not high when compared with blood cells, not all the detectors can receive the scattered Raman signal. Therefore, the distributed detection architecture suffers from incomplete information and it requires adjacent nano-sensors exchanging their data, which results in very complicated algorithm and it is out of the scope of this paper. Here, we consider the centralized architecture and the data fusion center can combine the sensed data. For instance, in the i^{th} sub-band, there are N_s detectors. The detected power is $\sum_{k=1}^{N_s} \hat{P}_k^{od}$ and the expected detected power is $N_s\mathbb{E}(P^d)$. Similarly, we can use (13) to find the estimated scattering coefficient.

V. NUMERICAL ANALYSIS

In this section, we numerically analyze the performance of the system. The parameters utilized are presented in Table I.

In the numerical simulation, we use a realistic Surface Enhanced Raman Spectroscopy parameters, which were measured through experiments [13]. The Raman shift is within [400,2300] cm^{-1} and the incident light wavelength is 755 nm. The particle density stands for the number of particles in a unit area. The transmission power of an emitter is set as 0 dBm. First, we set the molecule noise coefficient as 1×10^{-14} and vary

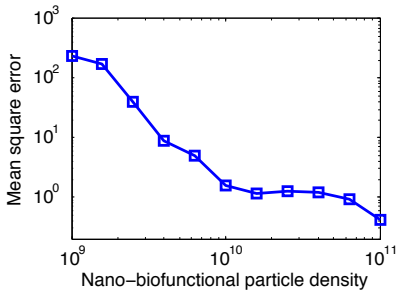

Fig. 5. Effect of particle density on estimation error.

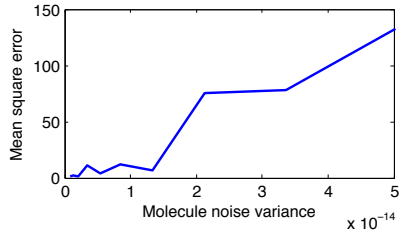

Fig. 6. Effect of molecule noise on estimation error.

the nano-biofunctional particle density. Since the shot noise power is almost a constant, it does not create randomness. As shown in Fig. 5, the increase of particle density can significantly reduce the mean square error. When the particle density is low, most of the sensors cannot detect scattered signal since there is almost no particles within its effective cone. Even worse, some of the sub-bands cannot detect any signal and thus the information of the sub-bands are missing. When it happens, we consider the sub-band has the same amplitude as its neighborhood sub-band. In Fig. 6, the particle density is kept as 10^{10} and the molecule noise is varied. As we can see, the molecule noise can dramatically affect the estimation accuracy as its power increases. With high molecule noise, the scattered signal by the targeted molecules can be submerged. In Fig. 7 and Fig. 8, we provide two examples of reconstructed Raman spectrums with different nano-biofunctional particle density. As can be seen from the figures, when particle density is large enough, the reconstructed spectrum matches well with the original spectrum. However, if the nano-biofunctional particle density is small, there is a large gap between the estimated spectrum and the original spectrum. Especially in Fig. 8, when Raman shift is larger than 1800 cm^{-1}, there is a flat area where the signal for the sub-bands cannot be detected due to the low density of the particle.

VI. Conclusion

Biosensing using nanotechnology can provide unprecedented accuracy for bio-detection of DNA and proteins, and disease diagnosis and treatment. Although conventional Raman spectroscopy can provide information at nanoscale in intra-body environment, the equipment utilized is bulky and expensive. In this paper, we propose a cooperative Raman spectroscopy using a large number of nano-transceivers on a ring. In this way, the detection device can be portable and affordable. The system architecture and operational framework are presented. Based on a stochastic system model, we provide a spectrum estimation and reconstruction method. The effect of the nano-biofunctional particle density and molecule noise

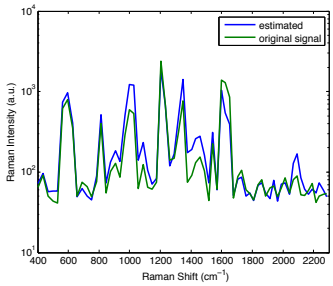

Fig. 7. Reconstructed Raman spectrum with 10^{11} particle density and 10^{-14} molecule noise coefficient.

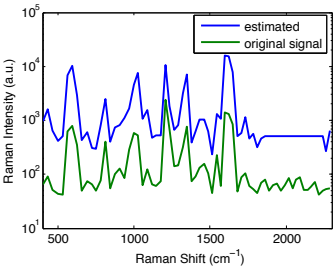

Fig. 8. Reconstructed Raman spectrum with 10^{9} particle density and 10^{-14} molecule noise coefficient.

are analyzed and the accuracy of the sensing system are evaluated. The results shown that the cooperative Raman spectroscopy is able to provide accurate estimation of the Raman spectrum, which can be utilized for molecule and chemicals identification.

References

[1] M. Sharon, A. K. Choudhary, and R. Kumar, "Nanotechnology in agricultural diseases and food safety," *Journal of Phytology*, vol. 2, no. 4, 2010.

[2] I. Kang, M. J. Schulz, J. H. Kim, V. Shanov, and D. Shi, "A carbon nanotube strain sensor for structural health monitoring," *Smart materials and structures*, vol. 15, no. 3, p. 737, 2006.

[3] Y. Hao and R. Foster, "Wireless body sensor networks for health-monitoring applications," *Physiological measurement*, vol. 29, no. 11, p. R27, 2008.

[4] I. F. Akyildiz and J. M. Jornet, "Electromagnetic wireless nanosensor networks," *Nano Communication Networks*, vol. 1, no. 1, pp. 3–19, 2010.

[5] I. Akyildiz, M. Pierobon, S. Balasubramaniam, and Y. Koucheryavy, "The internet of bio-nano things," *IEEE Communications Magazine*, vol. 53, no. 3, pp. 32–40, 2015.

[6] K. Vijayarangamuthu and S. Rath, "Nanoparticle size, oxidation state, and sensing response of tin oxide nanopowders using raman spectroscopy," *Journal of Alloys and Compounds*, vol. 610, pp. 706–712, 2014.

[7] L. Feng, Z. J. Wong, R.-M. Ma, Y. Wang, and X. Zhang, "Single-mode laser by parity-time symmetry breaking," *Science*, vol. 346, no. 6212, pp. 972–975, 2014.

[8] S. L. Jacques, "Optical properties of biological tissues: a review," *Physics in medicine and biology*, vol. 58, no. 11, p. R37, 2013.

[9] S. A. Prahl, M. Keijzer, S. L. Jacques, and A. J. Welch, "A monte carlo model of light propagation in tissue," *Dosimetry of laser radiation in medicine and biology*, vol. 5, pp. 102–111, 1989.

[10] L. Wang, S. L. Jacques, and L. Zheng, "Mcmlmonte carlo modeling of light transport in multi-layered tissues," *Computer methods and programs in biomedicine*, vol. 47, no. 2, pp. 131–146, 1995.

[11] J. C. Lin, *Electromagnetic fields in biological systems*. CRC press, 2011.

[12] H. Guo, P. Johari, J. M. Jornet, and Z. Sun, "Intra-body optical channel modeling for in vivo wireless nanosensor networks," *IEEE transactions on nanobioscience*, vol. 15, no. 1, pp. 41–52, 2016.

[13] N. Zhang, K. Liu, Z. Liu, H. Song, X. Zeng, D. Ji, A. Cheney, S. Jiang, and Q. Gan, "Ultrabroadband metasurface for efficient light trapping and localization: A universal surface-enhanced raman spectroscopy substrate for all excitation wavelengths," *Advanced Materials Interfaces*, vol. 2, no. 10, 2015.